Conceptual Missile Design Using Genetic Algorithms

Murray B. Anderson
Sverdrup Technology Inc./TEAS Group
308 West D. Avenue
Building 260
Eglin Air Force Base, FL 32542, USA

Executive Summary

This paper was written to show the potential of using an intelligent systems tool to rapidly conduct conceptual missile design studies. Rather than having separate teams of engineers developing/proposing discipline-specific designs (i.e. aerodynamics, propulsion, flight control system), a computer can quickly learn how to design a missile as an overall "system" to effectively defeat difficult targets. This paper was an invited paper presented at a joint NATO/Von-Karmen-Institute Workshop on Intelligent System held in Brussels, Belgium during May of 2002.

Abstract

For these preliminary design studies, a pareto genetic algorithm was used to manipulate a solid rocket design code, an aerodynamic design code, and a three-loop autopilot to produce interceptor designs capable of defeating two different target scenarios. The first scenario is a ground-launched interceptor engaging a high-speed/high-altitude target like a re-entry vehicle. The second scenario is an air-to-air engagement against a highly maneuverable target. Twenty-nine design variables were required to define the optimization problem, and two primary goals were established to access the performance of the interceptor designs. Design goals included minimizing both miss distance and intercept time. The genetic algorithm was able to quickly develop several basic types of designs that performed very well for the individual target scenarios.

Introduction

With the addition of guidance, an autopilot and an airframe with movable control surfaces, basic rocketry, expands into a more lethal and much more precise means of waging war. Rather than increasing the size of the warhead being delivered (to make-up for a loss in delivery accuracy), modern weaponeering has tended to use a small warhead coupled with an accurate control system. For ground launched systems, ideas such as "smart rocks" and "brilliant pebbles" that sprang from early Strategic Defense Initiative (SDI) research were based on the belief that the energy delivered by a small, fast moving projectile without an explosive could be as lethal as a less accurate system with an explosive warhead. Similarly for air-launched ground attack weapons, Vietnam proved that delivery accuracy was paramount to defeating tough targets. The Air Force subsequently devoted billions of dollars to the development of precise warhead delivery systems. The Persian Gulf War showed the benefit of these highly accurate weapon systems that were developed. While it is difficult to argue with the success of modern weapons, these systems share a common design philosophy that is somewhat lacking. When a system has a guidance system and autopilot, there is a tendency to compensate for less than stellar aerodynamic designs by shifting more and more of the delivery problems over to the autopilot. As a result, autopilots are typically very good and very robust, but the airframe and aerodynamics of the overall system are

Paper presented at the RTO AVT Course on "Intelligent Systems for Aeronautics", held in Rhode-Saint-Genèse, Belgium, 13-17 May 2002, and published in RTO-EN-022.

Report Documentation Page

Form Approved
OMB No. 0704-0188

1. REPORT DATE	2. REPORT TYPE	3. DATES COVERED
01 JUN 2003	**N/A**	**-**

4. TITLE AND SUBTITLE	5a. CONTRACT NUMBER
Conceptual Missile Design Using Genetic Algorithms	5b. GRANT NUMBER
	5c. PROGRAM ELEMENT NUMBER
6. AUTHOR(S)	5d. PROJECT NUMBER
	5e. TASK NUMBER
	5f. WORK UNIT NUMBER
7. PERFORMING ORGANIZATION NAME(S) AND ADDRESS(ES) **Sverdrup Technology Inc./TEAS Group 308 West D. Avenue Building 260 Eglin Air Force Base, FL 32542, USA**	8. PERFORMING ORGANIZATION REPORT NUMBER
9. SPONSORING/MONITORING AGENCY NAME(S) AND ADDRESS(ES)	10. SPONSOR/MONITOR'S ACRONYM(S)
	11. SPONSOR/MONITOR'S REPORT NUMBER(S)

12. DISTRIBUTION/AVAILABILITY STATEMENT
Approved for public release, distribution unlimited

13. SUPPLEMENTARY NOTES
See also ADM001519. RTO-EN-022, The original document contains color images.

14. ABSTRACT

15. SUBJECT TERMS

16. SECURITY CLASSIFICATION OF:			17. LIMITATION OF ABSTRACT	18. NUMBER OF PAGES	19a. NAME OF RESPONSIBLE PERSON
a. REPORT	b. ABSTRACT	c. THIS PAGE			
unclassified	**unclassified**	**unclassified**	**UU**	**28**	

almost an afterthought. Overall system performance and system capability, therefore, suffers because of the over-reliance on the autopilot to compensate for weaknesses in the aerodynamic performance of the weapon system. The goal of this research is to let an artificial intelligence tool, a genetic algorithm, design the aerodynamic shape while, at the same time, designing the propulsion system and determining key autopilot variables. This all-at-once approach to missile design is intended to provide a system capable of producing good aerodynamic shapes in addition to the good performance expected from an autopilot.

Following a discussion of the system components being manipulated by the genetic algorithm in this research, the operating modes of the genetic algorithm are discussed. Lastly, the results of the rapid design studies for the two target scenarios are presented.

Guidance Algorithm

Guidance is the first key component to accurately commanding a missile to a target. The guidance algorithm used in this study is standard proportional navigation (called ProNav). A ProNav system commands accelerations normal to line of sight between the missile and the target, proportional to the closing velocity (V_c) and the line of site rate ($\dot{\lambda}$). In equation form, this relationship is

$$\eta_c = N' V_c \dot{\lambda} \qquad \text{Equation 1}$$

where N' is the effective navigation ratio or gain. The closing velocity and line of sight rate are typically determined by a Doppler radar and seeker, respectively. For this research, it is assumed that there is a perfect seeker and a perfect radar system so that the target position and velocity are known exactly. For preliminary design studies, these two assumptions are appropriate. However, to make the autopilot performance variables (like damping ratio) more meaningful, the target position/velocity model was run at a slightly slower time step than the autopilot itself.

Before discussing the impact of the effective navigation ratio on the guidance system, it is appropriate to discuss how the commanded accelerations make their way into the missile control system. As a two-dimensional example, consider the yaw guidance plane shown in Figure 1. As this figure shows, from an inertial coordinate system viewpoint, the acceleration commands generated by ProNav are in the Earth-centered coordinate system (X,Y,Z) rotated through the line-of-sight angle. The commanded accelerations in the inertial axis system are then

$$a_X = \eta_c \cos(\lambda)$$
$$a_Y = -\eta_c \sin(\lambda)$$

These accelerations, and the ones from the corresponding X-Z plane, must be transformed into the missile body axis system before they can be used to move control surface to point the missile toward the target.

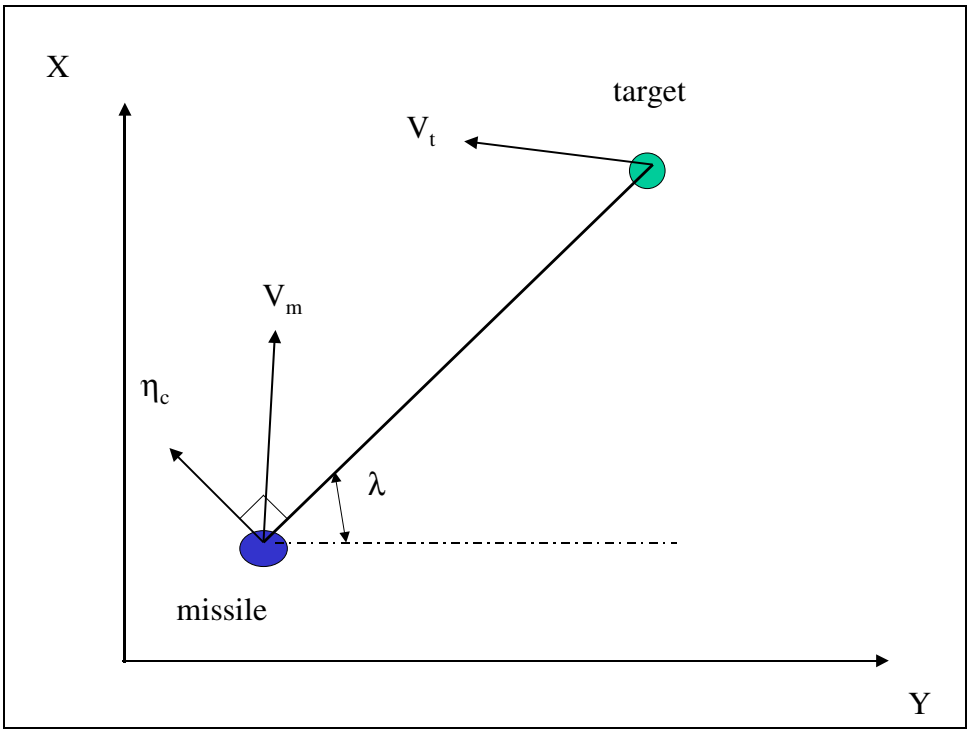

Figure 1. Guidance Command Schematic

The effective navigation ratio controls the behavior of the autopilot throughout the flight of the missile. Based on equation 1, it is obvious that, for a fixed closing velocity and fixed line-of-sight rate, higher effective navigation ratios mean higher commanded accelerations. Since it is the goal of the ProNav guidance law to eliminate the line-of-sight rate, higher effective navigation ratios translate into more active maneuvers early in flight in order to minimize the maneuvers near the end-game. For non-maneuvering targets, there is an obvious advantage to using a high effective navigation ratio. Typical ranges for this parameter are 3 to 5 (unitless) according to Zarchan[1] for tactical weapon systems. So, given this variation, the effective navigation ratio is a variable the genetic algorithm should determine.

As the missile enters the endgame maneuvers near the target, the line-of-sight rate will approach infinity as the missile passes (or passes through) the target and, therefore, the commanded accelerations will also approach infinity. It is common to limit the total acceleration commands (circular total acceleration commands) for flight systems and, for this study, the total acceleration was limited to 90 G's. Lateral accelerations greater than 90 G's would likely cause failure of the missile electronic components, if not failure of the structure itself.

Autopilot

The autopilot chosen for this study is the so-called three-loop pitch/yaw autopilot. This autopilot design was chosen because of its simplicity, because it is actively being used in several existing weapon systems, and because it is possible to analytically calculate the proper system gains (for all flight conditions) based on a few specified autopilot performance parameters. Since only the pitch and yaw channels are being modeled, the airframe is free to roll, and does so through induced roll rates as the missile pitches and yaws during intercept. This approach does reduce the turning efficiency of the missile but, as long

as the roll angles are tracked accurately, the autopilot is able to compensate. Often in preliminary design studies[2] the roll autopilot is modeled as a perfect stabilizer and is, therefore, neglected entirely. In this current research, inertial acceleration commands from guidance are simply rotated to the missile body axis system and the tail control surfaces respond with appropriate combined pitch/yaw commanded deflections to steer the missile to the target, regardless of the roll angle. The three loop autopilot (see Figure 2 for a schematic of one channel) takes acceleration commands from guidance and outputs the elevator/rudder commanded deflection angles that should be required in order to achieve the commanded accelerations. These tail control surface deflections produce a response through the airframe as a pitch/yaw rate and as a longitudinal/lateral acceleration. The rates and accelerations are fed back through the autopilot to dampen the system. For this study, it was assumed that the Inertial Measurement Unit (IMU)was perfect, meaning that the actual and measured accelerations and rates are identical. For simplicity, it is also assumed that the "perfectly measured" accelerations include appropriate translations to compensate for center-of-gravity movement as fuel is expended. In real systems, there will be lag and measurement error in the IMU, but for this preliminary design study, these simplifications are appropriate. The actuator was modeled as a 2nd order system[1] with a damping of 0.7 and a natural frequency of 125 rad/sec. These simplifications mean that the system is 5th order if the airframe is considered to be 2nd order response.

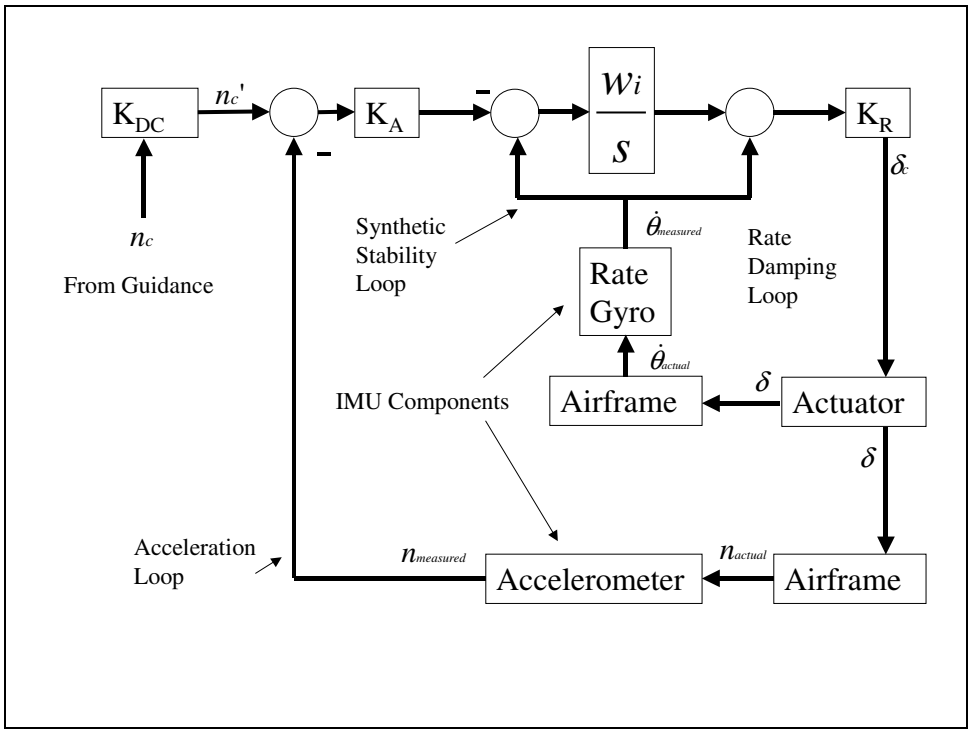

Figure 2. Basic Three-Loop Autopilot

As Figure 2 shows, there are plenty of feedback opportunities in the system to help maintain a robust controllable system for very diverse missile aerodynamic characteristics. The autopilot should be designed to provide a fast, well-damped response to acceleration commands. This task may seem easy at first, but consider what happens from the time a missile is launched to the time all the fuel is burned. It is very likely that the system center of gravity will have moved forward (stabilizing movement toward the nose), changing the airframe from a statically unstable system (center of pressure forward of the center of

gravity) to a stable system. For ground-launched missiles, the velocity of the missile may also have changed from 0 ft/sec to over 4,000 ft/sec and the altitude may have changed from sea level to over 100,000 feet. Throughout all these changes, the autopilot must adapt or the missile will be uncontrollable.

The three loops shown in Figure 2 serve specific purposes. The rate damping and synthetic stability loops provide proportional plus integral compensation, effectively damping the airframe poles[3]. The synthetic stability loop was originally added to compensate for statically unstable airframes. The acceleration loop controls the lateral acceleration of the missile. The autopilot gains are K_{DC}, K_A, ω_i, and K_R. All that needs to be done is to calculate the appropriate values for these gains. One of the reasons for choosing the three-loop autopilot is that these gains can be determined analytically from the aerodynamics of the airframe and from some specified performance parameters for the autopilot. These performance parameters are the damping ratio (ζ), time constant (τ), and crossover frequency (ω_{cr}). The system-damping ratio governs the sensitivity of the system (i.e. small heading errors should not produce large elevator/rudder deflections) and limits overshooting the commanded acceleration to help protect the structural integrity of the system and the electronics. The time constant is a measure of how fast the system responds to acceleration commands. For example, a 0.3 second time constant means that 63 percent of the commanded acceleration should be achieved in the first 0.3 seconds. The crossover frequency (when gain falls below 0.0Db) is a measure of autopilot robustness when higher order dynamics are not modeled. Since the system analyzed here is a 5^{th} order system, the crossover frequency essentially determines how fast the autopilot responds during homing. Higher crossover frequency values mean a faster autopilot but, if the autopilot is too fast, it can cause instability in the actuator. A good rule of thumb[1] is that the crossover frequency should not exceed 1/3 of the bandwidth of the actuator. In this study, the actuator was assumed to have a natural frequency of 125 rad/sec and a damping of 0.7, so the highest crossover frequency that can be safely used should be around 41.66 rad/sec to maintain stability. This particular instability is the reason why, in preliminary design studies, determining a good estimate of the crossover frequency can only really be done with a 5^{th} order system or higher. Evaluation of 3^{rd} order systems (perfect actuator) is usually a first step to analyzing a 5^{th} order system (actuator included), followed by an 11^{th} order system that includes actuator dynamics, IMU response, and structural dynamics[2].

The equations that determine the four autopilot gains (at a single flight condition) from the aerodynamics and autopilot performance parameters are omitted in this discussion. These equations can readily be obtained from multiple sources. , However, it should be noted that Nesline[2] provides general equations that work well even for very unstable missiles, while Zarchan[1] does not. The basic premise of these equations is that the aerodynamic derivatives (like $C_{m\alpha}$ and $C_{m\delta}$) and expected aerodynamic damping provide a means of determining the linear response that a system is capable of delivering at a given dynamic pressure. If the system response can be estimated, appropriate gain schedules can be developed to achieve the desired autopilot performance levels.

It should also be noted that, for the ground launch case, the autopilot is not activated until 0.4 seconds into the flight to give the system time to generate enough speed to make fin commands meaningful.

Aerodynamics Code

Washington[4] developed AeroDesign, the aerodynamic prediction methodology used as the basis for this study. AeroDesign was modified to include two axial force considerations that were not part of the original software. First, the fineness ratio of the nose of the missile is compared to a Sears-Haack[5] body and, if the nose is not slender enough, a drag penalty

proportional to the nose bluntness is added to the baseline axial force coefficient. The second axial force coefficient correction was implemented to correct for cases where the rocket nozzle exit diameter actually exceeds the diameter of the body.

AeroDesign was further modified to provide aerodynamic damping derivative estimates and linear aerodynamic coefficient contributions for deflected control surfaces in the pitch and yaw planes in a format and flight condition range compatible with a guided six-degree-of-freedom simulation.

Rocket Performance Code

The solid rocket performance software used in this study is an erosive burning star grain design program that is suitable for preliminary design studies. There are some fundamental assumptions made in the formulation of the software that are suitable for rapid evaluation of preliminary design. The major assumptions are:

1. The pressure varies throughout the chamber, however, the pressure is calculated only at the head end (P_1) and at the grain end (P_2). The chamber pressure (P_{CH}) is then defined as the average of these two pressures.
2. The burn rate of the propellant also varies over the entire surface and is subject to erosive burning. The burning rate at any point can be defined as $r = aP_{CH}^{\ n}\left(1 + k \cdot V\right)$, where k, a, and n are burning rate constants. Since the chamber pressure is calculated only at the head end where V_1 equals 0, and at the aft end of the grain, where V equals V_2, the velocity is averaged to calculate an average erosive burning rate.
3. The grain burns on the edges normal to the centerline of the rocket only (i.e. no end-burning so x_{gl} is constant) at the average burning rate.
4. The flow is isentropic between the aft end of the grain and the throat.
5. The flow obeys the perfect gas law.
6. The chamber pressure varies with time, but is essentially constant during the discharge of a single particle.
7. The flow is one-dimensional and steady.
8. There is no deformation of the propellant due to acceleration, pressure, or viscous forces.
9. The temperature is uniform throughout the grain, but the grain is temperature sensitive (this is a fuel characteristic).

The rocket motor to be designed by the genetic algorithm has certain definable characteristics such as the strength of the combustion chamber material, which should be known before the design process begins. For this study, the following rocket characteristics were used:

1. Propellant is ammonium perchlorate (80%).
2. Initial temperature of the propellant is 20°C.
3. The design chamber pressure (i.e. maximum chamber pressure for case structural design) is 3000 psi. Chamber case thickness is determined by using a factor of safety of 1.5 given this maximum chamber pressure.
4. The allowable stress in the case is 195,000 psi.
5. The factor of safety is 1.5.
6. The case is made of a steel alloy with a density of 0.28 lbm/in^3.

7. The nozzle is made of an aluminum alloy with a density of 0.19 lbm/in^3.

For this study, ammonium perchlorate (80%) was chosen but there is no reason why the propellant choice could not be another design parameter if there is a database of propellant burning characteristics available. For ammonium perchlorate, the erosive burning rate constant k is 1.0E-4 sec/ft, and the burning rate constants a and n are 0.15 and 0.4, respectively.

Six-Degree-of-Freedom (6-DOF) Simulation

The equations of motion used in this 6-DOF were obtained from Etkin[6] assuming that (1) the missile structure is essentially rigid, (2) there are no rotating masses internal or external to the missile, and (3) there are no significant cross products of inertia. Using Etkin's notation, longitude is measured positive from west to east, which is opposite from conventional world maps. The simulation was modifed so that even though Etkin's coordinate system is used exactly, the output of the simulation is converted to standard world map definitions to avoid confusion. Also consistent with Etkin, the standard Eulerian definitions of Φ, Θ, and Ψ were used. To avoid gimbal lock (θ=90 deg) concerns, quaternions were used instead of the standard Euler angles during the integration process. However, all output was converted from quaternions to Euler angles for output.

The conventional body-fixed acceleration and moment equations were modified to include aerodynamic damping terms and contributions due to control surface deflections. For this study, a tail-control missile was assumed but there is no reason why a canard-control system could not also be analyzed. The definitions used for the control surface contributions to the aerodynamic coefficients were as follows:

1. positive elevator commands produce positive normal force contributions and negative pitching moment contributions
2. positive rudder commands produce positive side force contributions and negative pitching moment contributions

For a 5th order system, 19 differential equations must be solved simultaneously (15 for the quaternion system of equations and 4 for the elevator and rudder).

Link to GA: GA with Aerodynamics, Propulsion, Six-DOF, Guidance, Autopilot, and Target

Linking the separate software codes to the genetic algorithm was done in a modular fashion so that other modules could be later substituted for the ones used in this study. The genetic algorithm passes all design variables down to the Six-DOF via one subroutine call statement (single line of interface). The Six-DOF then calls the other components, including the mass properties routine that calculates the component inertias and the center of gravity for the system. For this study, the payload was assumed to weigh 50 lbf and the electronic components/actuators weighed an additional 50 lbf.

Variables Governing Design

There are nine variables that govern the solid rocket motor design, fourteen variables that govern the external shape of the vehicle, two variables that control the launch angle (verticality and heading), three variables that define the autopilot performance, and one variable to set the effective navigation ratio or gain. Figure 3 shows the external geometry variables, with the exception that the nozzle exit radius is actually determined from the expansion ratio (A_e/A^*), which is one of the solid rocket motor design variables. Though the

nozzle is shown, it is merely for visualization purposes. The nozzle actually resides within the total length of the missile. The nozzle exit radius is not, however, free from external aerodynamic considerations since there is a substantial drag penalty that can be incurred if the nozzle exit radius exceeds the body radius. Hopefully, the genetic algorithm will learn to design the rocket motor and external shape cooperatively so that good thrust levels are obtained without incurring a drag penalty. Basically then all outer body dimensions are controlled by the genetic algorithm, from the nose length to the nozzle exit radius. Figure 4 and Figure 5 show the nine solid rocket motor design variables that are also part of the design process, with (A_e/A^*) being one of those variables.

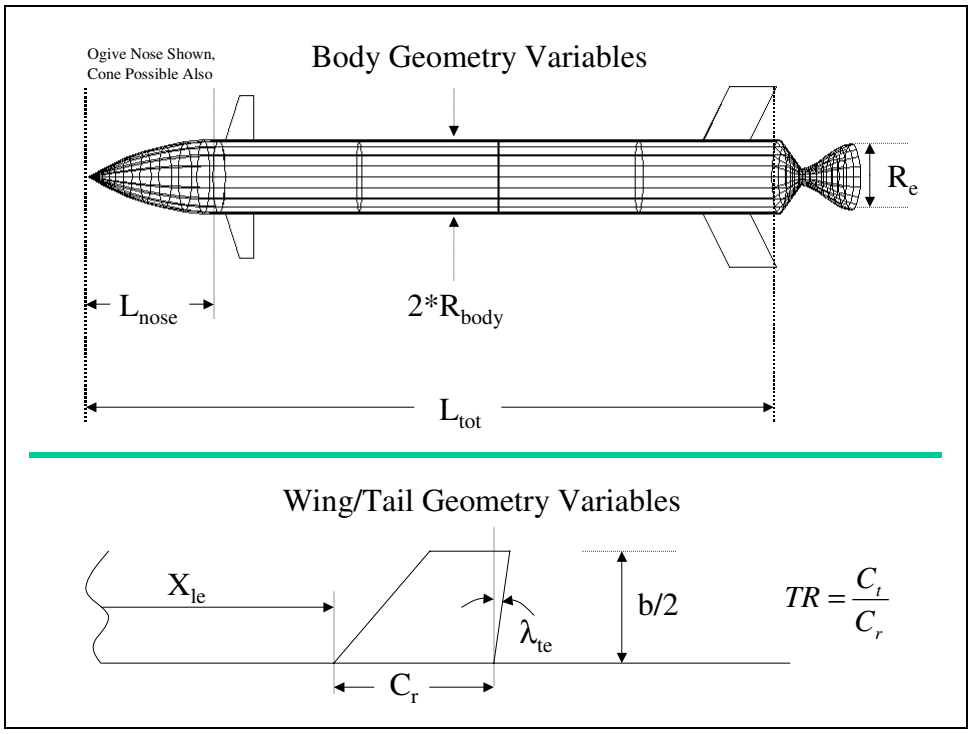

Figure 3. External Shape Design Variables

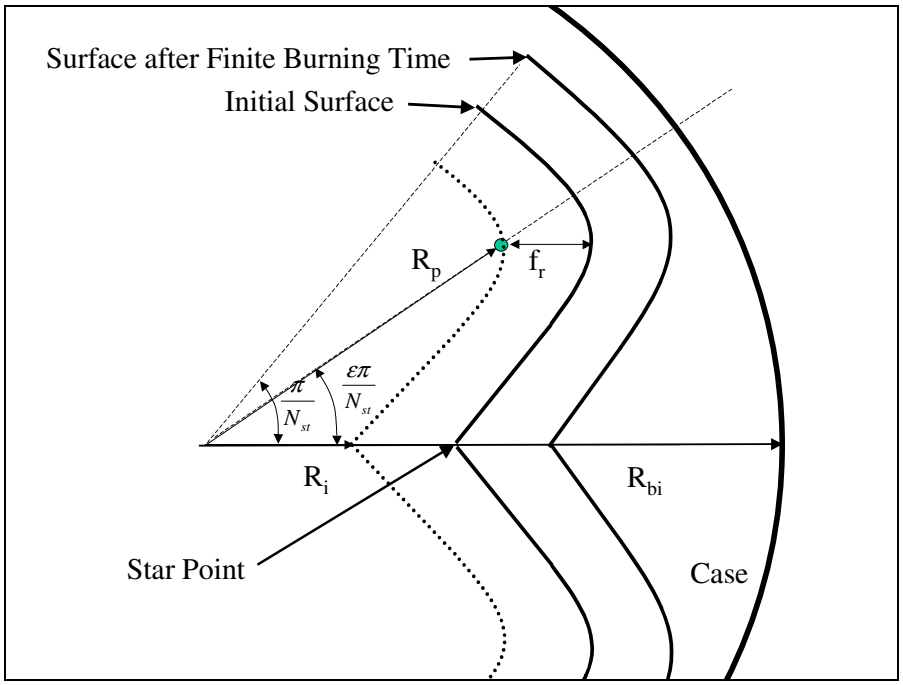

Figure 4. Solid Rocket Motor Grain Design Variables

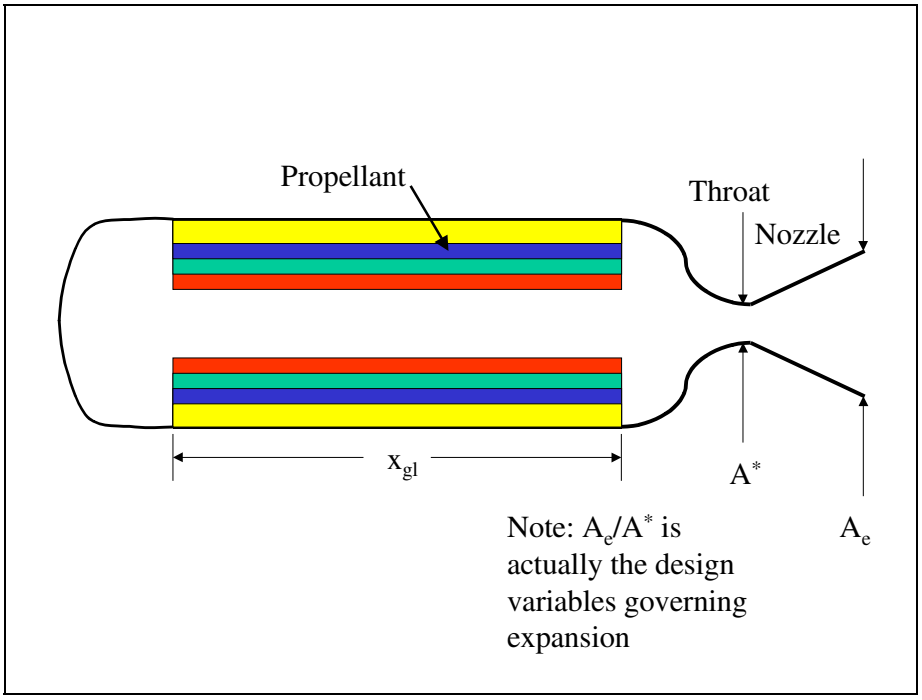

Figure 5. Solid Rocket Motor Grain Length, Throat Diameter, and Expansion Ratio

Table 1 formally defines each design variable and Table 2 shows the minimum, maximum, and resolution that is desired for each variable. The maximum, minimum, and resolution

dictate the size of the optimization space. In genetic algorithm terms, the number of genes in each chromosome is defined as:

$$number\ of\ genes = \sum_{n=1}^{\substack{number \\ of \\ parameters}} \left(INTEGER\left[\frac{LN\left(\frac{\max_n - \min_n}{resolution_n} \right)}{LN(2)} \right] + 1 \right)$$

The genetic algorithm requires parameter bounds and resolutions only and, from this table, it is obvious that a very broad range of designs is possible. In fact, the specified bounds and resolutions means that 2^{175} possible designs exist. The size of this problem is tremendous, especially when the number of atoms in the universe is estimated at 2^{266}.

Table 1. Design Variables for Guided Systems

Variable Name	Definition (units)
R_{bi}	Grain outer radius, also the rocket motor case inner radius (inches)
R_p	Outer star radius (inches)
R_i	Inner star radius (inches)
x_{gl}	Grain Length (inches)
N_{st}	Number of star points
f_r	Fillet radius (inches)
ε	Angular fraction (rad)
D^*	Diameter of the throat (inches)
R_{exp}	Nozzle expansion ratio (area of throat/area of exit)
Nose	1 – Ogive, 2 – Cone
L_{nose}	Nose Length (inches)
L_{tot}	Total Body Length excluding nozzle (inches)
R_{body}	Body radius (inches)
b_w	Exposed semi-span of wing (inches)
C_{rw}	Wing Root chord (inches)
λ_{tew}	Wing Trailing Edge Sweep Angle (deg)
TR_w	Wing Taper ratio (C_t/C_r)
X_{lew}	Distance from nose tip to wing leading edge (inches)
b_t	Exposed semi-span of tail (inches)
C_{rt}	Tail Root chord (inches)
λ_{tet}	Tail Trailing Edge Sweep Angle (deg)
TR_t	Tail Taper ratio (C_t/C_r)
X_{let}	Distance from nose tip to tail leading edge (inches)
θ	Euler Vertical Launch Angle (θ=90 would be vertical (deg))
Ψ	Euler Launch Heading Angle (Ψ=90 would be East (deg), 0 would be North)
ζ	Damping Ratio
τ	Time Constant
ω_{cr}	Crossover Frequency
N'	Effective Navigation Ratio or Gain

Table 2. Maximum, Minimum, and Resolution of Variables for Guided Systems

Parameter	Minimum	Maximum	Resolution	Number of Genes
R_{bi}	2.0	10.0	0.02	9
R_p	0.2	9.9	0.02	9
R_i	0.1	9.5	0.02	9
x_{gl}	50.0	200.0	1.0	8
N_{st}	3	10	1	3
f_r	0.05	1.0	0.01	7
ε	0.25	1.0	0.01	7
D^*	0.1	9.0	0.01	10
R_{exp}	1.0	20.0	0.2	7
Nose	0	1	1	1
L_{nose}	20.0	90.0	5.0	4
L_{tot}	50.0	450.0	10.0	6
R_{body}	3.0	20.0	1.0	5
b_w	0.0	80.0	1.0	7
C_{rw}	0.0	80.0	1.0	7
TR_w	0.0	1.0	0.1	4
λ_{tew}	0.0	44.0	2.0	5
X_{lew}	20.0	200.0	5.0	6
b_t	0.0	80.0	1.0	7
C_{rt}	0.0	80.0	1.0	7
TR_t	0.0	1.0	0.1	4
λ_{tet}	0.0	44.0	1.0	5
X_{let}	200.0	400.0	5.0	6
θ	5.0	90.0	1.0	7
ψ	0.0	180.0	1.0	8
ζ	0.2	1.0	0.05	4
τ	0.1	0.9	0.1	3
ω_{cr}	10.0	100.0	5.0	5
N'	2.0	5.0	0.1	5

Mode of Operation of Genetic Algorithm

The controls for the genetic algorithm used in this study were fairly common. The number of population members was limited to 150 because of computer run time considerations. Generally, the more population members the better, but when running a 6-DOF thousands of times it was necessary to limit the population size to less than the number of genes. Historically, pareto GA's have been run with more population members than genes to help maintain good diversity in the presence of competing goals.

The following table lists all the genetic algorithm operating modes/parameters that were used for this study.

Table 3. Genetic Algorithm Controls for Guided Missile Cases

Mode/Variable	Value
Number of Goals	2
Steady State Algorithm	False
Elitist	True
Creep Mutation	True
Remove Duplicates	True
Number of Members of the Population	150
Crossover Rate	90%
Mutation Rate	0.2%
Creep Rate	2%
Selection Process	Tournament
Crossover	Single Point

Design Conflict Checking

Some obvious geometrical checks were used to keep the genetic algorithm from expending computational resources on designs that were not practical. Seven separate checks were made as follows:

1. Outer rocket motor case radius cannot exceed body radius
2. Rocket motor grain length cannot exceed body length
3. Tail control surfaces cannot be coincident with, or in front of, wing
4. Tail control surfaces cannot overhand the aft end of the missile
5. Wing cannot overhand nose portion
6. Based on the specified payload and electronic weights and densities, as well as the rocket motor size, the total volume of the missile must be able to house these components
7. Tail control surfaces must be located such that the actuator hinge line (assumed to be at the 50% location of the tail root chord) can be placed at, or very near, the rocket motor throat. Since the actuators take up a considerable volume, it is logical that they would be placed near the throat of the nozzle.

If any of these conflicts occur, the genetic algorithm sends back extremely poor performance values in each goal area, so that it will learn not to try these designs in the future.

Thermal and Structural Considerations

The 6-DOF software calculates stagnation temperature at each time step based on Mach number and altitude (standard atmosphere is assumed). If the stagnation temperature ever exceeds 2500 degrees Rankine, then the system is assumed to fail because of thermal loads.

The structural considerations are manifested in the strength of the wings and tails since these are obvious weak points. Wing and tail loads during flight are used to calculate root bending moments and bending stresses. If the bending stresses ever exceed 185,000 psi (typical for stainless steel), the wing or tail surfaces fail and the flight is terminated at that point. The wing joints are assumed to be rigidly connected to the missile body along the entire root chord. Each actuator-controlled tail surface is assumed to be mounted on a 1.25-inch diameter stainless steel rod. The genetic algorithm must learn to design systems that will not fail either thermally or structurally.

The Target

The two targets specified for this research are vastly different. The first is a fast point-mass ground-attack re-entry vehicle like a SCUD missile. The second is a highly maneuverable air-to-air target capable of random 5-15G's maneuvers every 0.1 seconds. The target subroutine defines initial positions, velocities, and accelerations for the target and performs simple Euler integration on the equations of motion to update the target's position and velocity in time. For the random maneuvering target scenario, each missile design was flown against 10 different random targets and the miss distances and intercept times were averaged.

Launch Conditions

The launch velocity (for the assumed launch aircraft) was specified to be 700 ft/sec at 5000 feet altitude. An ideal launch was assumed so there were no initial angular rates imparted to the missile. The launch aircraft heading and pitch attitude were variables to allow the genetic algorithm find the best way to design, as well as launch, the missile.

Goals for Guided Interceptor

The goals against both targets were to minimize both miss distance and intercept time. Given the pareto genetic algorithm, to win the tournament selection process, a competing solution must be better than a competitor in both goal areas simultaneously.

Results: Ground Launched Interceptor

With the design problem and parameters completely defined, the pareto genetic algorithm was executed until satisfactory missile performance was obtained. Figure 6 shows the convergence history for each goal. As this figure shows, it took the genetic algorithm 12 generations (1800 attempts) before it found a design that was capable of even lifting off the ground. Designs that could not produce thrust were given a miss distance error of 1E+5 so that the genetic algorithm would learn that these were very bad designs. Once the genetic algorithm learned how to produce thrust, the miss distance fell to 298,000 feet at generation 12. This large miss distance was due to tail fin failure just after lift-off. Luckily, within two more generations (generation 14), the genetic algorithm found a design that would not fail structurally or thermally. This design flew to within 30 feet of the target. Such a large change in performance is rather unusual and highlights what can happen if the right crossover or mutation occurs at the right place and at the right time. This is not to say that the best design of generation 12 actually produced the design at generation 14, but that the

surviving genes from generation 12 combined with other survivors and produced a 2nd generation descendant with substantially improved performance. These two designs are substantially different (see Figure 7). The generation 12 design had a radius of 8.5 inches and a takeoff weight of over 2500 pounds. The generation 14 design had a radius of 6.3 inches and a takeoff weight of 1700 pounds. The design at generation 14 had much smaller tail surfaces, so these surfaces were able to maintain their structural integrity. The generation 12 tail surfaces failed within 1/2 second of autopilot initiation.

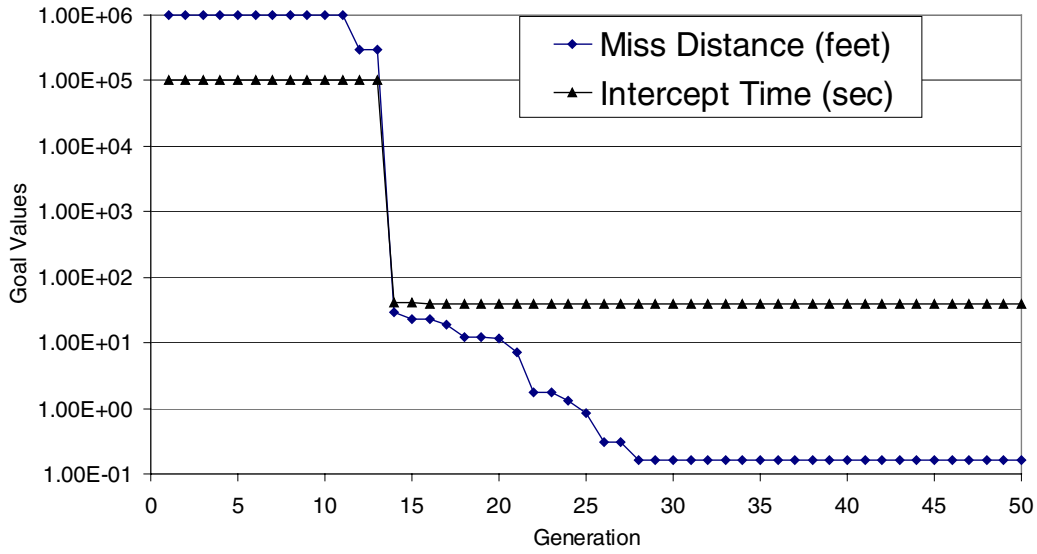

Figure 6. Convergence History for Guided Interceptor Goals

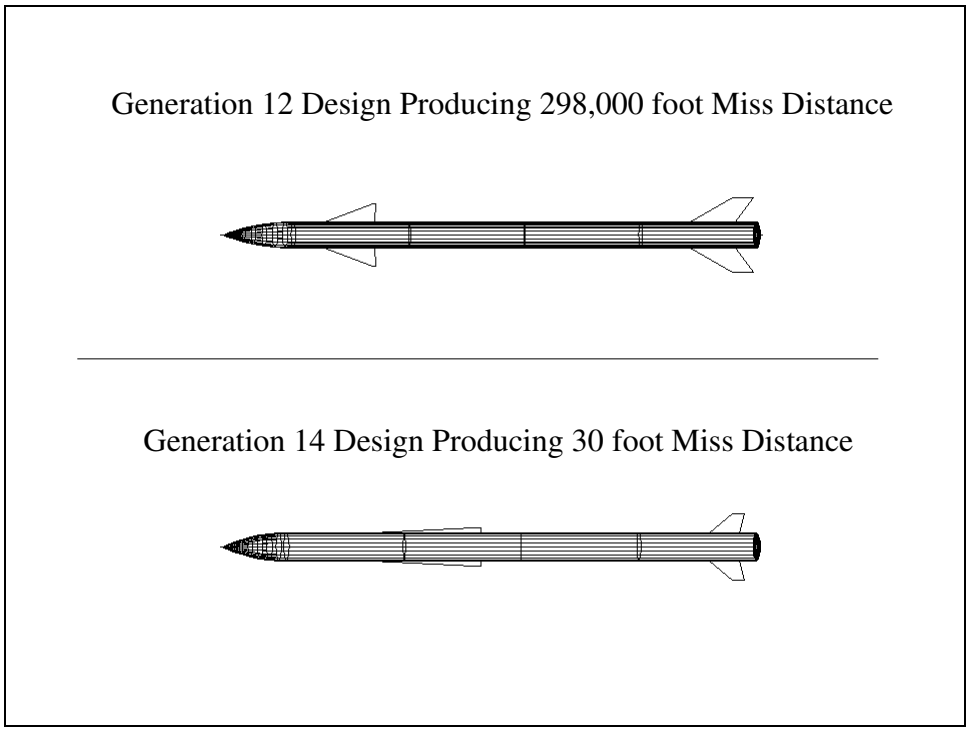

Figure 7. Design Changes from Generation 12 to Generation 14

The minimum miss distance continued to improve from generation 14 to generation 28, falling to within 0.16 feet. Given the time step that was used for the last one-second of the engagement, the minimum miss distance could only be 0.1 feet at best. So, it is fair to say that the accuracy of the system was near a maximum by generation 28. Prior to the last one-second of flight, the time step was such that the system accuracy could be no better than approximately 5 feet. A larger time step saves considerable computer run time and, for preliminary design efforts, saving computer time is important. No further improvement in the minimum miss distance was seen between generation 28 and generation 50.

Though difficult to see in Figure 6 because of the scale, the minimum intercept time fell from 41.6 seconds to 38.5 seconds between generations 14 and 50, and the takeoff weight fell from over 2500 pounds to less than 700 pounds. The convergence figure does not imply that the 700 pound rockets actually hit the targets, nor does it imply that the designs that pulled less than 0.2 G's hit the target. Rather, this figure merely shows that, within the 150 members of each population, the lightest rocket capable of lift-off weighed less than 700 pounds and at least one rocket never pulled more than 0.2 G's during its flight. Analysis of these particular systems showed that the light rockets did not fly very far and that the low-G rockets barely lifted off.

Since there were multiple goals involved in the design process, it is appropriate to examine the history of each goal area through the generations. Figure 8 shows miss distance and intercept time for several generations. It is clear that more and more members of the population maneuver closer and closer to the target as the generations progress. In generation 14, 36 members of the population (36 out of 150) had a miss distance within 100 feet. By generation 50, 124 members of the population reached within 50 feet of the target. By inspection it is also clear from this figure that intercept time falls appreciably between generations 30 and 50, even though the two populations have similar miss distance distributions. Of solutions with a 5-foot miss distance, intercept times varied between 38.8 seconds and 42.3 seconds.

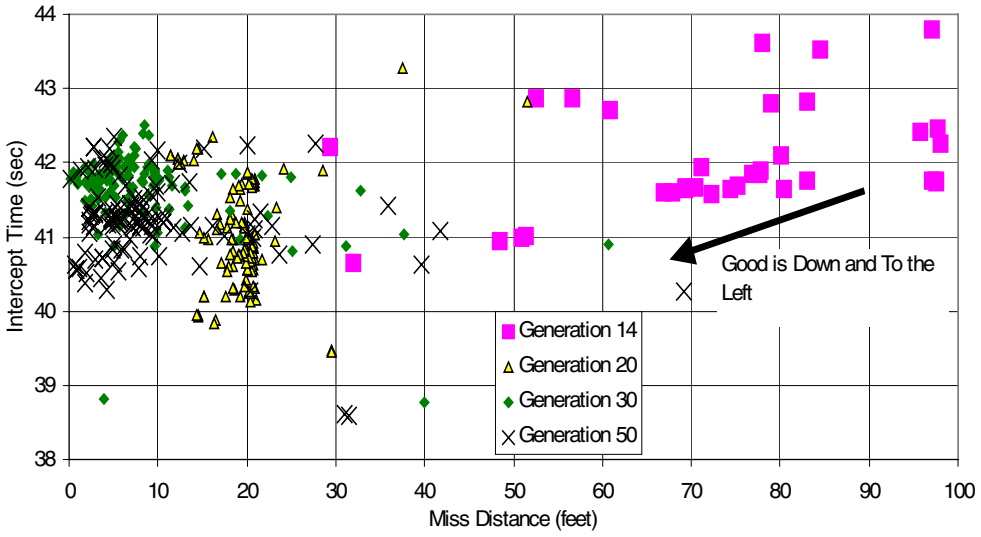

Figure 8. Miss Distance and Intercept Time: Generations 14, 20, 30, and 50

Figure 9 shows the prevalent time constants and damping ratios that dominated generation 50. There are clearly not 150 individual points (representing members of the population) on this figure because, by generation 50, many members of the population were using exactly the same damping ratios and time constants. High system damping is obviously preferred.

This result should be expected since overshooting acceleration commands is not a desirable missile flight characteristic because it wastes energy. The preferred time constants were in the 0.5 to 0.6 second range, which is very reasonable since the target is not conducting evasive maneuvers to escape the interceptor. Missiles that are designed to intercept high-G (9-G's is typical) maneuvering targets have time constants near 0.2 to 0.3 seconds so that they can quickly respond to target evasive tactics.

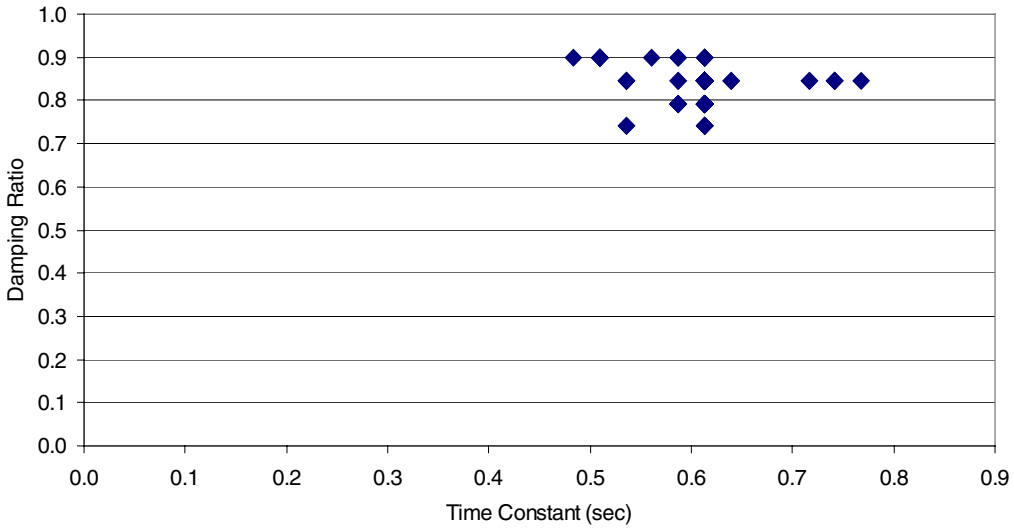

Figure 9. Generation 50 Time Constants and Damping Ratios

Figure 10 shows the proportional navigation gains and crossover frequencies that dominated the population at generation 50. Fairly high navigation gains (4.7-5.0) dominated the population, which means that system quickly tried to minimize heading errors. Low values of the navigation gain, in the 2.0 to 3.5 range, would tend to delay the correction of heading errors. For high altitude intercept missions, it makes sense to take out heading errors early in the flight, rather than waiting until the altitude is such that system responsiveness suffers from the lack of air density (i.e. dynamic pressure). The dominant crossover frequencies were between 20 and 30 rad/sec. This result is not too surprising since the highest value that could safely be used[1] was roughly 41.66 rad/sec, which corresponds to 1/3 of the bandwidth of the actuator used in this study.

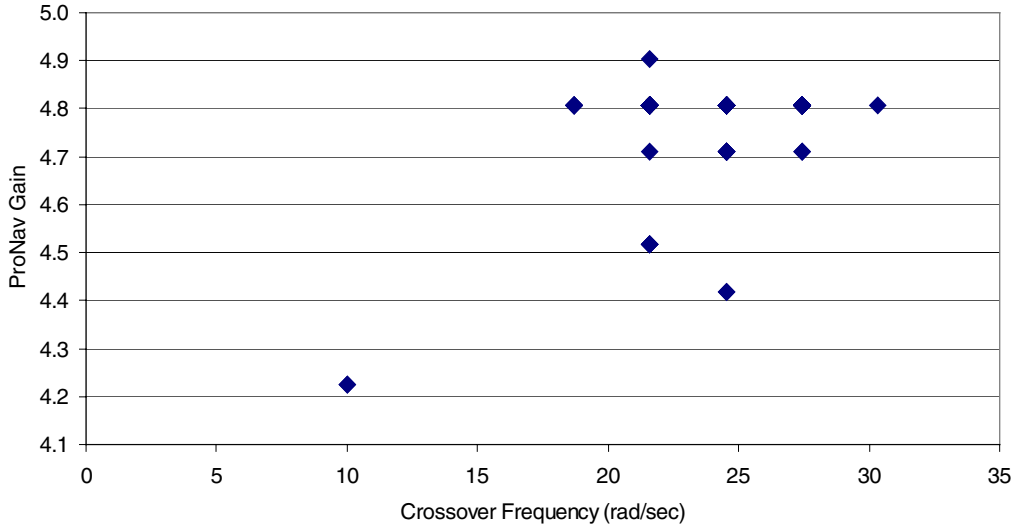

Figure 10. Generation 50 Proportional Navigation Gains and Crossover Frequencies

Although neither the launch angles nor the autopilot performance parameters show great variation among the members of the population, the actual missile designs produced during the solution process are quite diverse. Figure 11 through Figure 14 show the diversity that exists in a population. The first generation 30 design that is shown happens to be the design that intercepted the target substantially faster that it's contemporaries (recall Figure 8). This nine-pointed star design has fairly small wings and the tail control surfaces are well ahead of the aft end of the rocket. The nose is also fairly blunt. This missile is, however, able to fly to within four feet of the target more quickly than the others. The time constant, damping ratio, and crossover frequency for this design was 0.69 seconds, 0.85, and 21.6 rad/sec, respectively. Certainly such a long time constant could help explain some of the miss distance. Smaller time constants help make the system more responsive. The navigation gain was 4.52, which will tend to make the system minimize heading errors as early in the flight as possible when there is sufficient dynamic pressure to make steering easier. The designs shown in Figure 11 include forward and aft wing placements, low and high wing taper ratios, swept and unswept wing/tail trailing edges, and cone and ogival noses that have both high and low fineness ratios. The solid rocket motors themselves are fairly consistent, having a large initial burning area (9 and 10 point star grains) and large combustion chamber volumes.

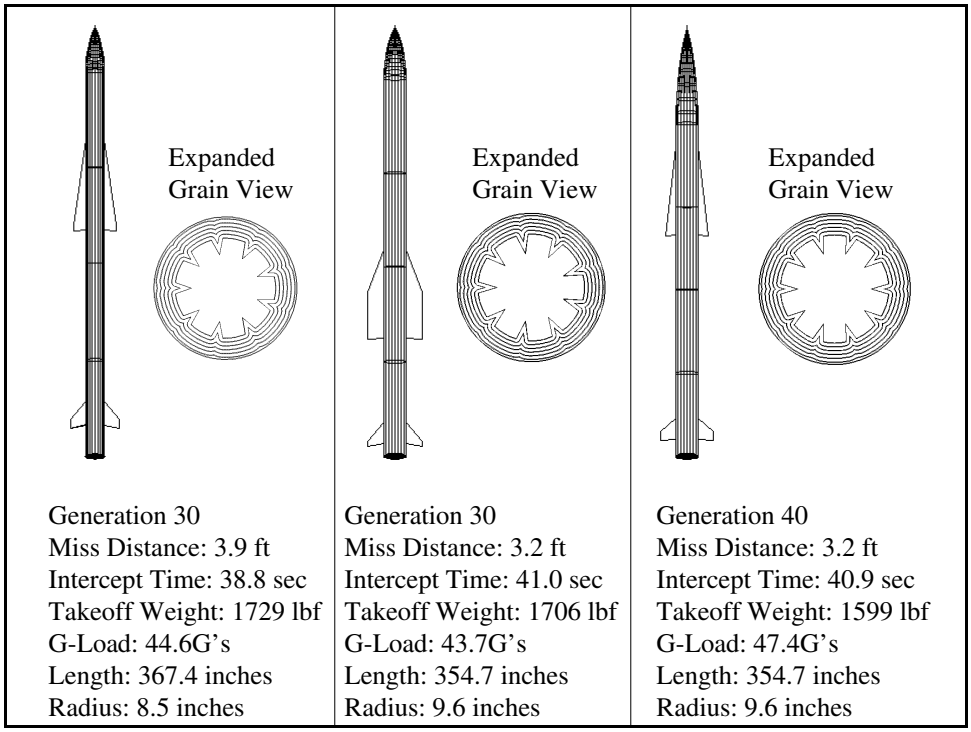

Figure 11. Sample Designs from Generations 30 and 40

The designs shown in Figure 12, Figure 13, and Figure 14 all come from generation 50, the final generation, and are segmented into designs that have miss distances less than 3 feet, 2 feet, and 1 foot respectively. Not all the designs that meet these accuracy criteria are shown. These particular designs are merely representative of some of the more accurate designs in the population. By generation 50, the genetic algorithm has found two basic classes of external designs that work fairly well: highly tapered, small semi-span, forward-placed wings and moderately tapered, moderate semi-span, aft-placed wings. The genetic algorithm found that large semi-span designs produce large bending moments (which tend to cause structural failure), so wing areas were held at reasonable levels by increasing the root chord. The tail surfaces are fairly similar, though the placement of the surfaces varies slightly as does tail size. The placement of the control surfaces dictates where the throat of the rocket motor is placed (to make room for the actuators within the missile body), so the length of the nozzle expansion region varies. In no case, however, did the actual exit area exceed the diameter of the missile body. Designs yielding nozzle exit radii exceeding the radius of the missile body would produce excess drag, and the genetic algorithm learned to avoid these types of designs. There is a chance, therefore, that the rocket motor exhaust pressure would not match local ambient conditions very well during the boost phase of the interceptor, and this question will be examined in more detail later. First though, the rocket motor grain designs appear to be very similar, but Figure 12 shows examples of 8, 9, and 10 pointed star grains. A common feature in generation 50 was also present in generation 30 and generation 40, namely large initial burning areas and large combustion chambers.

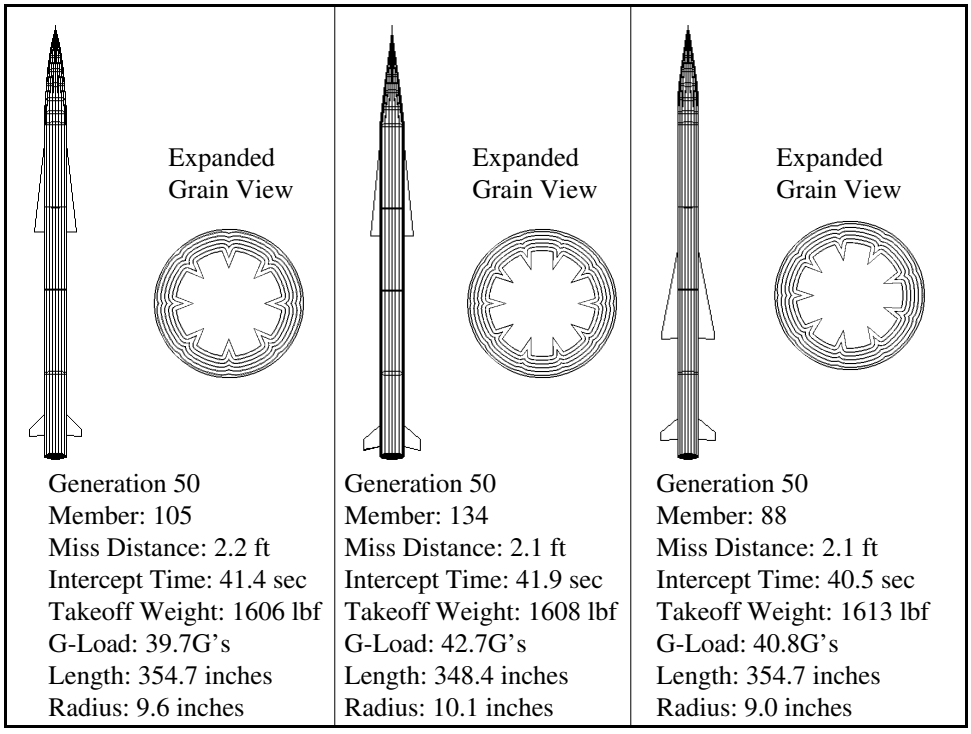

Figure 12. Three Generation 50 Designs with Miss Distances Less Than Three Feet

Nose shapes also continue to vary between ogive's and cone's, although it appears that the ogive nose exists in the more accurate examples. Physical sizes and takeoff weights of the interceptors are very similar, as are intercept times and maximum G-loads. The three best designs (in terms of miss distance only) all had 9-pointed star grains, but the wing sizes and locations still vary significantly. It is also interesting to note that these designs all had nose shapes that were fairly blunt compared to the other designs that were slightly less accurate. These nose shapes were not blunt enough to incur a drag coefficient penalty larger than 0.012 based on a Sears-Haack body, so an examination of the aerodynamic data for these shapes revealed that the net effect of the change in the nose length was to move the center of pressure farther forward very slightly (an average of approximately 1.5 inches) over all flight conditions. This center of pressure movement helped reduce the static margin at rocket motor burnout, thereby increasing maneuverability at the coast condition without seriously impacting maneuverability during rocket motor burn.

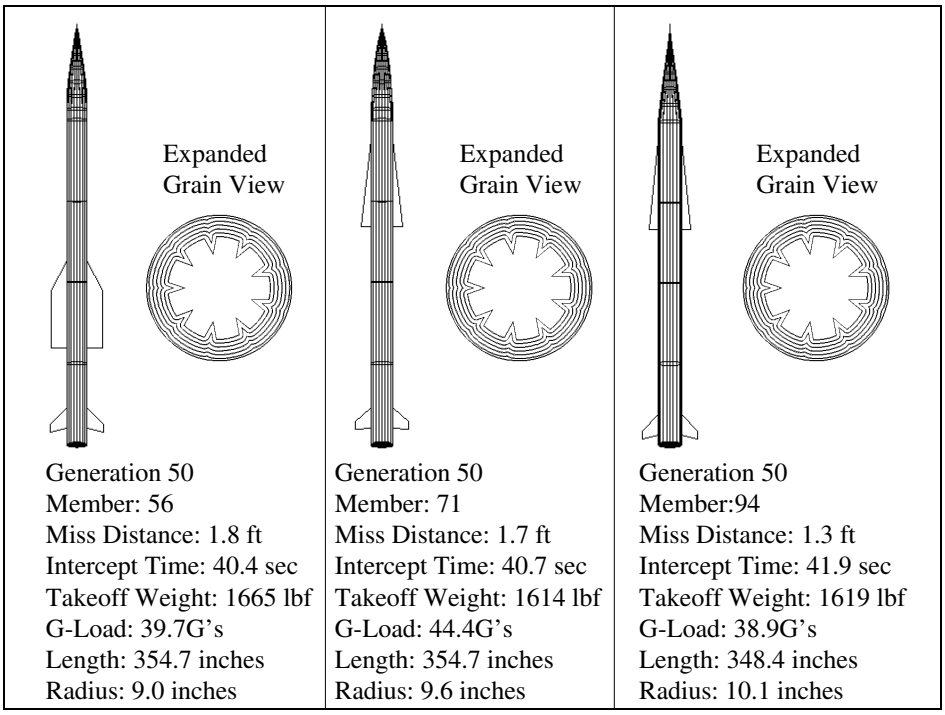

Generation 50 Member: 56 Miss Distance: 1.8 ft Intercept Time: 40.4 sec Takeoff Weight: 1665 lbf G-Load: 39.7G's Length: 354.7 inches Radius: 9.0 inches	Generation 50 Member: 71 Miss Distance: 1.7 ft Intercept Time: 40.7 sec Takeoff Weight: 1614 lbf G-Load: 44.4G's Length: 354.7 inches Radius: 9.6 inches	Generation 50 Member:94 Miss Distance: 1.3 ft Intercept Time: 41.9 sec Takeoff Weight: 1619 lbf G-Load: 38.9G's Length: 348.4 inches Radius: 10.1 inches

Figure 13. Three Generation 50 Designs with Miss Distances Less Than Two Feet

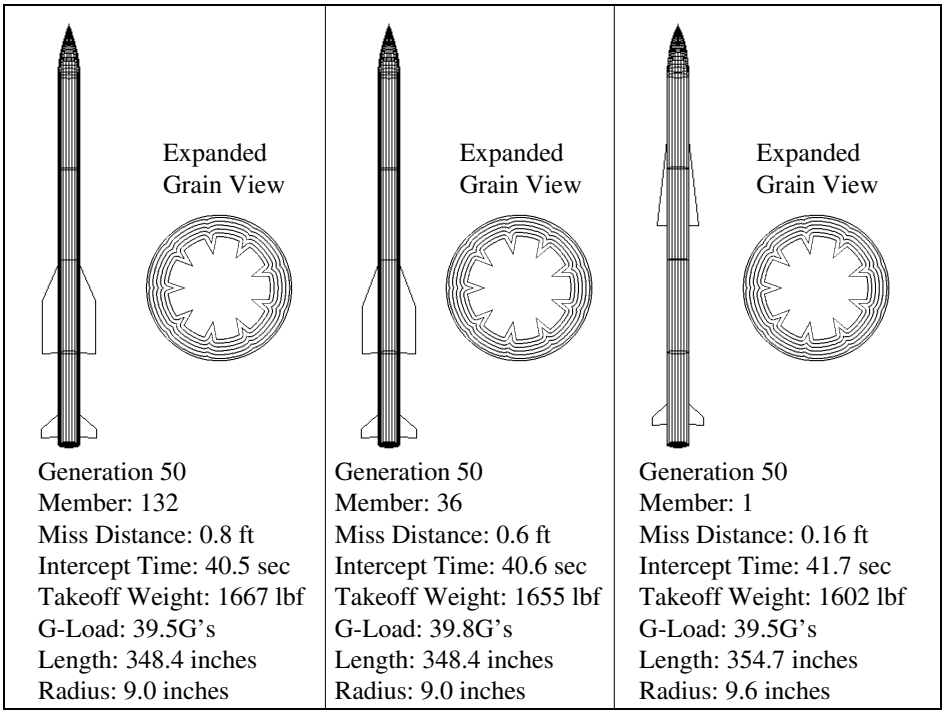

Generation 50 Member: 132 Miss Distance: 0.8 ft Intercept Time: 40.5 sec Takeoff Weight: 1667 lbf G-Load: 39.5G's Length: 348.4 inches Radius: 9.0 inches	Generation 50 Member: 36 Miss Distance: 0.6 ft Intercept Time: 40.6 sec Takeoff Weight: 1655 lbf G-Load: 39.8G's Length: 348.4 inches Radius: 9.0 inches	Generation 50 Member: 1 Miss Distance: 0.16 ft Intercept Time: 41.7 sec Takeoff Weight: 1602 lbf G-Load: 39.5G's Length: 354.7 inches Radius: 9.6 inches

Figure 14. Three Generation 50 Designs with Miss Distances Less Than One Foot

It is obvious from Figure 15 why the interceptor is able to build up Mach 4 speeds so fast. The initial take-off thrust is nearly 64,000 lbf and, as the sharp star points burn off, the thrust reduces to approximately 37,000 lbf before increasing again as the burning area begins to

increase during the final burning phase. The chamber pressure is nearly 2,000 psi initially, which is well within the 3,000 psi limit of the rocket motor case. Higher chamber pressures may be more efficient in terms of utilizing the case weight that is present (less rocket case steel could have been used had thickness been a design variable), but given the fact that the missile nearly reaches the thermal limit, this may be a case where not violating the thermal barrier was more important than a few extra pounds of weight.

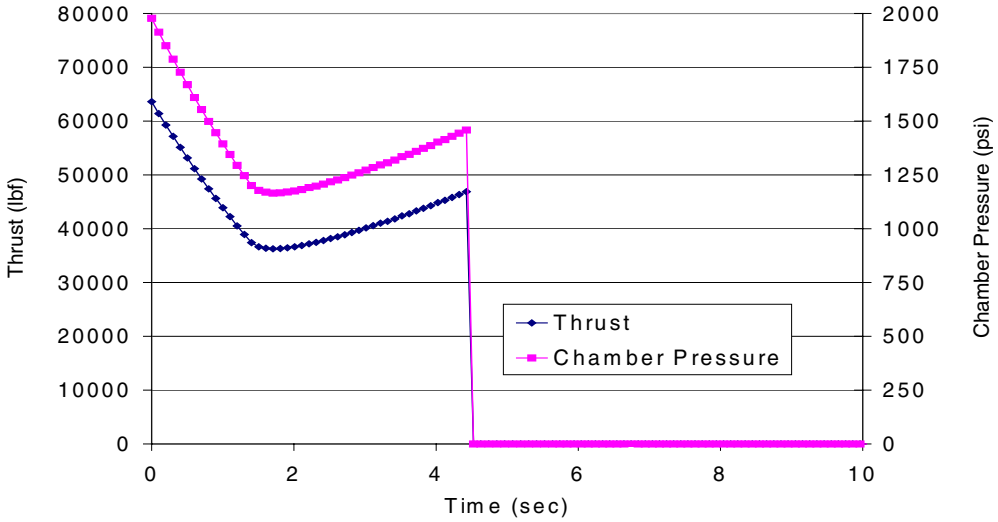

Figure 15. Thrust and Chamber Pressure History

One clear measure of thrust efficiency, however, is the ratio of the nozzle exit pressure to the local ambient pressure (P_e/P_a). A ratio of 1.0 is the most efficient, and Figure 16 shows that the genetic algorithm did a good job of compromising the exit pressure ratio to be both above and below the ideal ratio during the burn. Since a variable nozzle exit area was not possible with this system, the ideal ratio cannot be maintained. It is remarkable, however, that the genetic algorithm was able to design the rocket motor throat/exit expansion ratio so that a reasonable pressure ratio was obtained while keeping the nozzle exit radius within the body case radius to avoid a drag penalty. The ability of the genetic algorithm to simultaneously work on multiple goals while under multiple constraints/penalties makes it a robust "hands-off" design tool. The fact that the genetic algorithm also seems to yield good results for implicit (not-stated) performance goals, such as maintaining a nozzle exit pressure ratio near 1.0, also highlights the value of the technique.

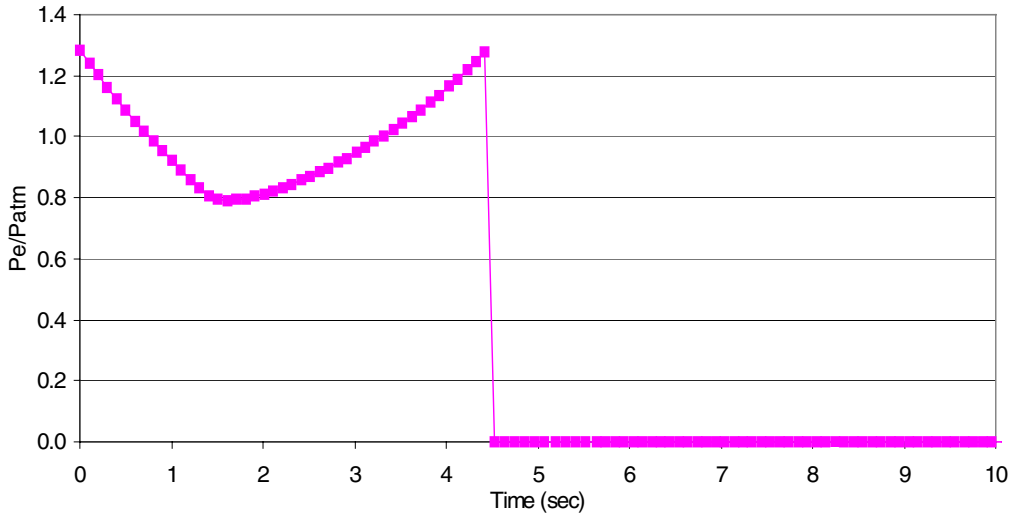

Figure 16. Exit Pressure Ratio History

Results: Air-to-Air Interceptor

Figure 17 shows the convergence history of the best performer in the two goal areas. There was a major performance improvement at generation 108, and continued learning until generation 150. Recall that each potential design was flown against 10 separate random targets, so it should be expected that there would be some noise in the miss distance goal even though elitism was chosen.

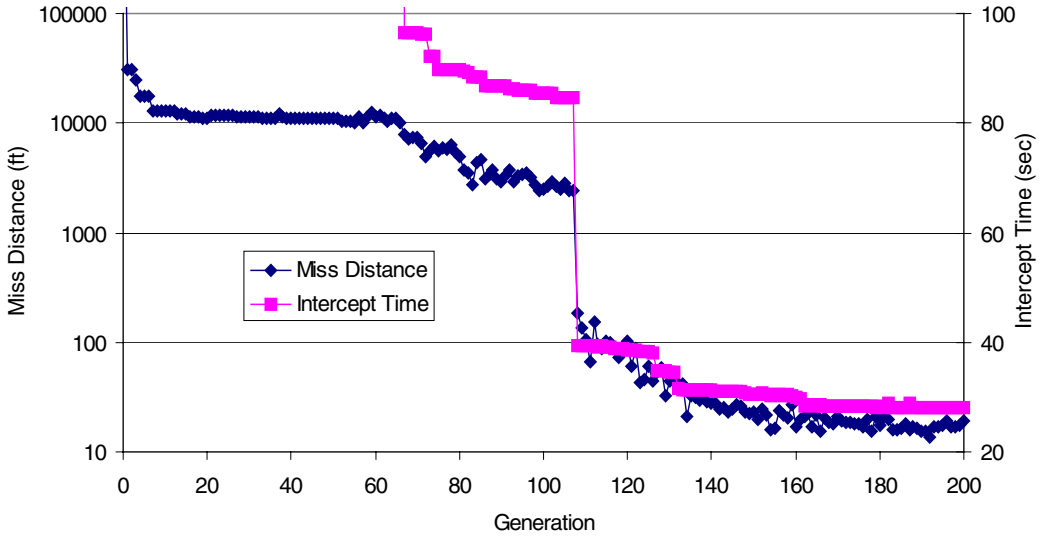

Figure 17. Convergence History of Best Performer in the Two Goals

Figure 18 shows population diversity in the two goals at several generations. There is very clear performance improvement in both goals from generation 120 to generation 150. More and more of the population members began to take on the successful characteristics of their ancestors, and, therefore, the number of competitive solutions began to increase. This is most obvious when looking at the sheer number of solutions that are competitive in generation 150 versus generation 120.

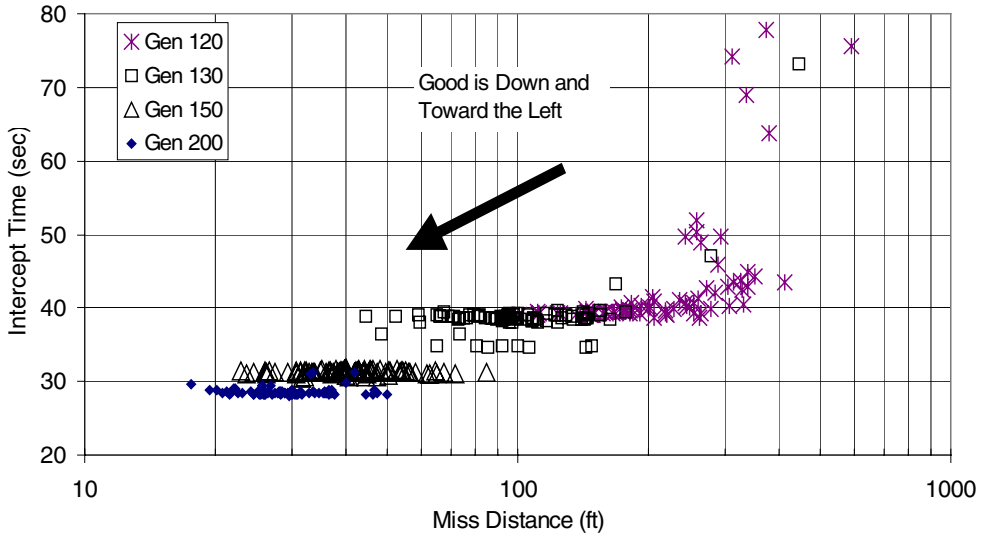

Figure 18. Intercept Time and Miss Distance Diversity

Some of the more competitive missile designs from generation 200 are shown in Figure 19. The most obvious feature of these designs is the large wing/tail surfaces. For high maneuverability, large surfaces are needed since thrust vectoring is not currently part of the design process. Wing placement is also very far forward in order to enhance turning ability. As the rocket motor burns the center of gravity of the missile moves forward, so a forward wing placement helps offset some of the inherent stability due to center of gravity motion. It is interesting to note that a circular cross section was preferred for the solid grain, meaning a progressive thrust profile. One reason for choosing a progressive thrust profile could be that, since the launch point was at 5,000 feet (altitude) and the target was at 20,000 feet, it might be beneficial from a thermal viewpoint to delay achieving maximum Mach number until reaching an altitude with a lower static temperature.

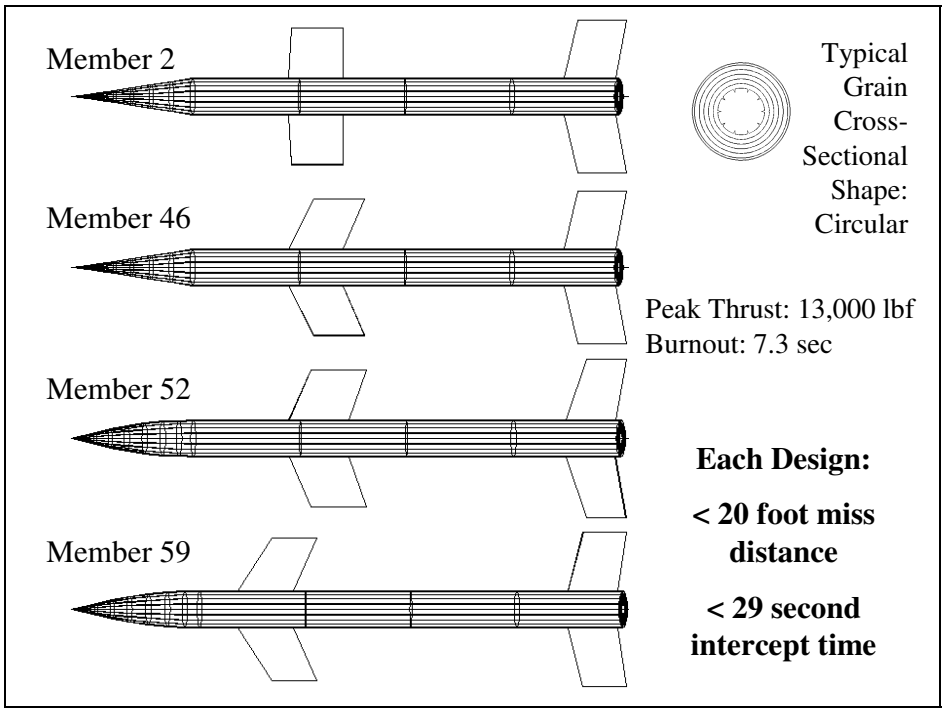

Figure 19. Various Missile Designs from Generation 200

Figure 20 shows the Mach number and temperature profile for one of the flights for the first missile (member 2) shown above. As you can see, the genetic algorithm was pushing the thermal limit in order to minimize the intercept time, so having a progressive thrust profile probably helped keep the missile from exceeding the thermal limits. Prior to burnout, the missile had climbed to approximately 10,000 feet and had a Mach number near 4.5. Had the missile been at 5,000 feet at Mach 4.5, it would have exceeded the thermal limit of 2500 degrees Rankine by over 25 degrees.

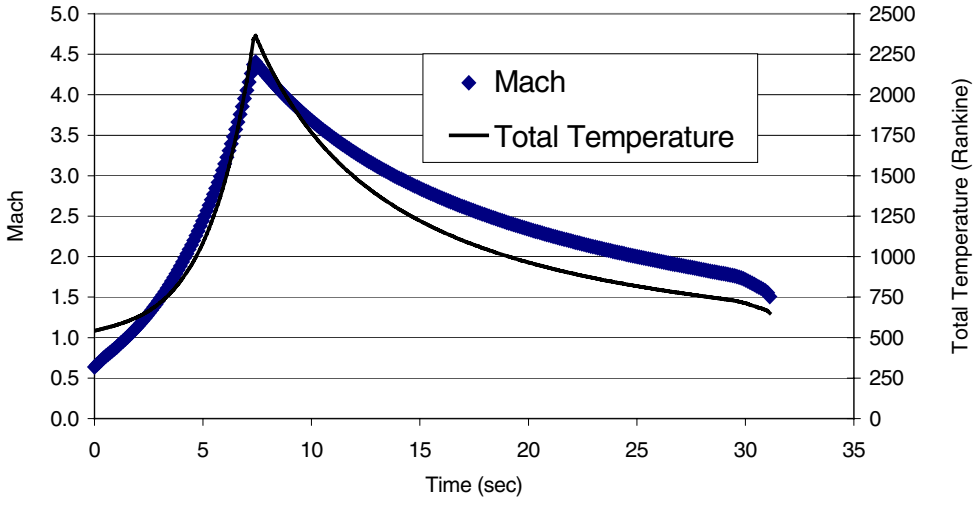

Figure 20. Mach Number and Total Temperature Profile for a Rapid Intercept Case

These acceleration histories were achieved with the types of damping ratios, time constants, navigation gains, and crossover frequencies shown in Figure 21 and Figure 22. The time constants concentrated around 0.37-0.47 seconds. Recall that there are 100 actual points on these figures, though it appears that there are less because many points are the same. In fact, of the 100 solutions at generation 150, over 80 of them used a time constant between 0.37 and 0.42 seconds. The favorite damping range was from 0.63 to 0.88, with a fairly even distribution of solutions in this range. This is moderate damping.

The Navigation gains are fairly conventional for air-to-air interceptors (4.5-4.9), but many of the specified crossover frequencies are very high. There is a cluster of solutions within the conventional air-to-air missile range, between 47-54 rad/sec. But there is another cluster between 85 and 94 rad/sec that is close to the actuator natural frequency of 125 rad/sec. Analyses of these high crossover frequency cases shows that, although they are only marginally stable at certain flight conditions, they are (on average) just as accurate as the solutions having lower crossover frequencies. They do, however, have lower stability margins and are more prone to excitation at certain airspeeds. Since there was no goal established to assess stability per se, it is natural that these types of solutions would survive since their performance in the two stated goals was comparable to the more stable solutions.

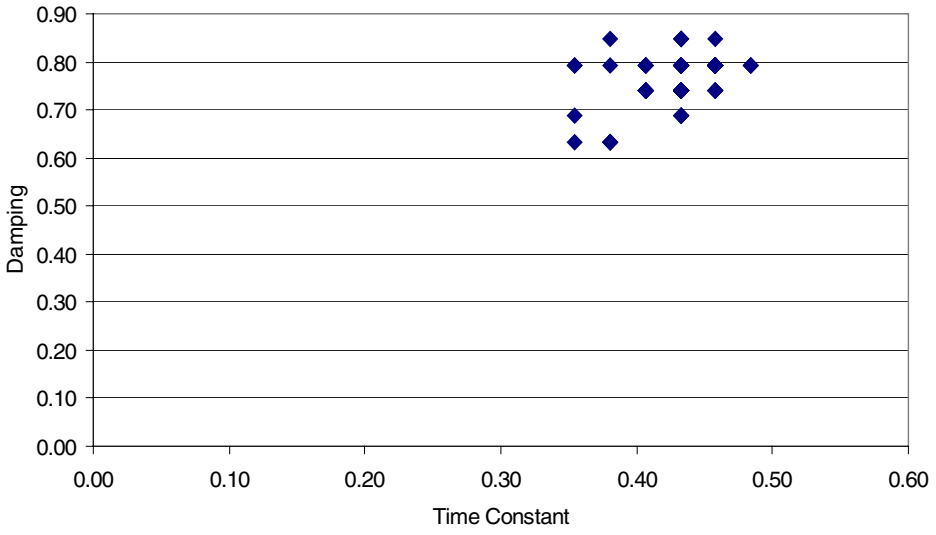

Figure 21. Generation 100 Time Constants and Damping Ratios

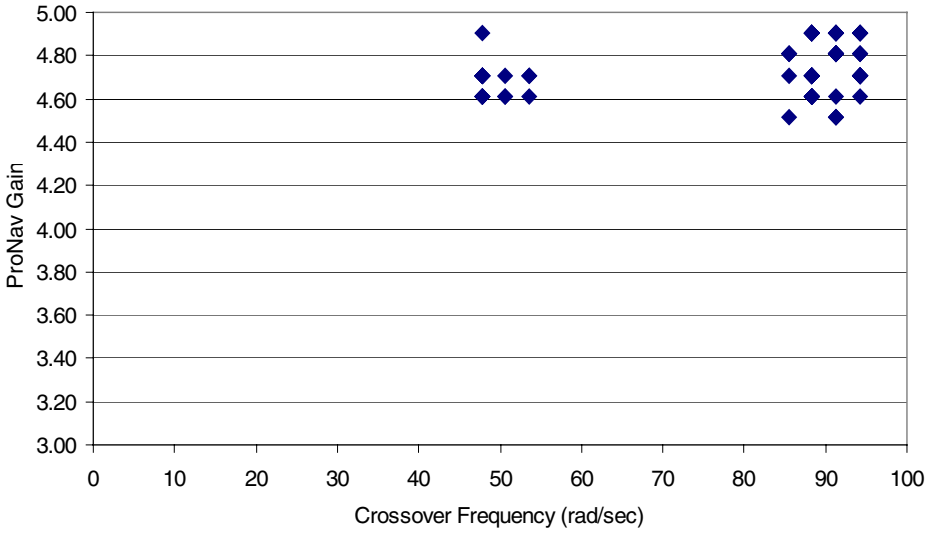

Figure 22. Generation 100 Navigation Gains and Crossover Frequencies

Computer Run Time

The 200 generations presented here required 10 days of CPU time on a Silicon Graphics R-10000 processor. The R-10000 is approximately the same speed as a 400 MHz Pentium II processor.

Conclusions

The pareto genetic algorithm is well suited to designing complete interceptor systems consisting of propulsion, aerodynamics, and autopilot modules. This work has shown that an all-at-once design process, controlled by the proper artificial intelligence tool, is not only possible, but much faster than iteratively designing each subsystem component into a workable package. Simple constraints, such as the thermal limits and structural integrity calculations used in this work, provide a means of injecting real-world considerations into the design process. Even with diverse performance modules and diverse goals, the genetic algorithm was able to learn how to design around the constraints while achieving good performance in overall system goals. In both the difficult high-altitude/high-speed engagement scenario and the highly maneuverable air-to-air target scenario, the genetic algorithm developed multiple designs capable of close intercept.

The basic three-loop autopilot is ideal for preliminary design studies. Improvements such as thrust compensation could, and should, be included when the design process moves beyond the preliminary stage. The analytic determination of gains, and gain schedules based on Mach number and altitude, have made three-loop autopilots very popular in current missile systems. The basic proportional navigation guidance algorithm used here worked well, but it is likely that performance could be improved by using multiple algorithms during different phases of flight to correct, for example, the adverse acceleration commands at low launch speeds.

References

[1] Zarchan, Paul, *Tactical and Strategic Missile Guidance*, 3rd Edition, Volume 176, American Institute of Aeronautics and Astronautics, 1997.
[2] Nesline, F.W. and Nesline, M.L., "How Autopilot Requirements Constrain the Aerodynamic Design of Homing Missiles," Conference Volume of 1984 American Control Conference, San Diego, CA, June 6-8, 1984.
[3] Stallard, D.V., "An Approach to Autopilot Design for Homing Interceptor Missiles," AIAA- 91-2612-CP, AIAA Guidance and Control Conference, 1991.
[4] Washington, W. D., "Missile Aerodynamic Design Program," 1980, 1990.
[5] Ashley, H., and Landahl, M., *Aerodynamics of Wings and Bodies*, Dover Publications Inc., New York, New York, 1965.
[6] Etkin, Bernard. *Dynamics of Atmospheric Flight*, John Wiley and Sons, 1972.

This page has been deliberately left blank

Page intentionnellement blanche